

Numerical Analysis of InGaAsP Carrier-depletion Optical Modulator on III-V CMOS Photonics Platform

Naoki Sekine¹, Jaehoon Han^{1,2}, Mitsuru Takenaka^{1,2} and Shinichi Takagi^{1,2}

¹ Univ. of Tokyo, 7-3-1 Hongo, Bunkyo-ku, Tokyo, 113-8656, Japan, ² JST-CREST.

Phone: +81-3-5841-6733, FAX: +81-3-5841-8564, E-mail: sekine@mosfet.t.u-tokyo.ac.jp

Abstract

The carrier-depletion InGaAsP optical modulator on the III-V CMOS photonics platform is numerically analyzed. The InGaAsP optical modulator exhibits 5 times greater modulation efficiency than the Si optical modulator with keeping comparable insertion loss.

1. Introduction

Si photonics is a promising option to realize low-power optical interconnection for datacenters. In Si photonics, the large refractive index contrast between Si ($n=3.4$) and SiO₂ ($n=1.9$) makes it possible to strongly confine light in Si and to fabricate ultra-small optical components. Among Si photonics components, Si optical modulators are one of the fundamental building blocks [1]. Most of Si optical modulators are based on the plasma dispersion effect. However, the weak plasma dispersion effect in Si results in the low modulation efficiency [2]. Since the plasma dispersion effect is proportional to an inverse of effective mass, according to the Drude model, III-V semiconductors such as InGaAsP are expected to possess greater plasma dispersion effect than Si. To realize Si-photonics like III-V photonics, we have proposed the III-V CMOS photonics platform by using the III-V on Insulator (III-V-OI) wafer [3]. On this platform, passive devices [4,5] and active devices including carrier-injection optical switches [6], photodetectors [7], laser diodes [8] have been reported. However, no high-speed modulator has been reported yet on the III-V-OI wafer.

In this paper, we have proposed a carrier-depletion InGaAsP optical modulators with a lateral PN junction on the III-V CMOS photonics platform as shown in Fig. 1. By using TCAD simulation, we have numerically analyzed the InGaAsP optical modulator on the III-V CMOS photonics platform.

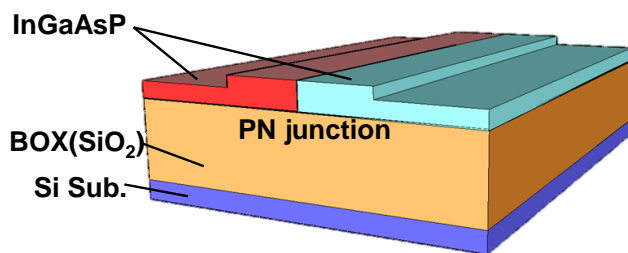


Fig. 1 Schematic of InGaAsP carrier-depletion modulator on III-V-OI wafer.

2. Device structure and analysis method

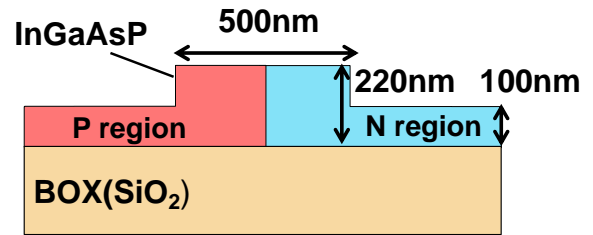


Fig. 2 Cross-sectional structure of InGaAsP optical modulator.

III-V semiconductors are known to have several free-carrier effects including the plasma dispersion effect, free-carrier absorption, band filling effect, band gap shrinkage, and intervalence band absorption which contribute to refractive index change and absorption coefficient change [9,10]. Except for the plasma dispersion effect, these effects directly contribute to absorption coefficient change, but also contribute to refractive index change through the Kramers-Kronig relationship. Especially the band filling and bandgap shrinkage effects become larger when the bandgap energy becomes small. In this paper, we consider optical modulators operated at a wavelength of 1550 nm. Hence, among III-V semiconductors, InGaAsP with a bandgap wavelength of 1370 nm is assumed to gain maximum refractive index change with negligible band-edge absorption. The InGaAsP with such a bandgap energy is easily grown on an InP wafer because of the lattice matching.

A cross-sectional structure of the proposed InGaAsP optical modulator is shown in Fig. 2. A 220-nm thick InGaAsP layer is bonded on a 2- μ m thick SiO₂ buried oxide layer. A 500-nm wide rib waveguide with a 100-nm thick slab is assumed. A lateral PN junction is formed at the center of the waveguide for carrier depletion. The doping density of the P and N regions is assumed to be $5 \times 10^{17} \text{cm}^{-3}$, $1 \times 10^{18} \text{cm}^{-3}$ or $2 \times 10^{18} \text{cm}^{-3}$. We also consider a Si optical modulator with the same device structure for comparison.

The modulation characteristics are analyzed by using Sentaurus TCAD in conjunction with an optical mode solver based on the finite-element method. First, a carrier density distribution is calculated by TCAD at each reverse voltage. Then, the effective refractive index change and absorption change for the fundamental optical mode are obtained to calculate modulation efficiency and insertion loss.

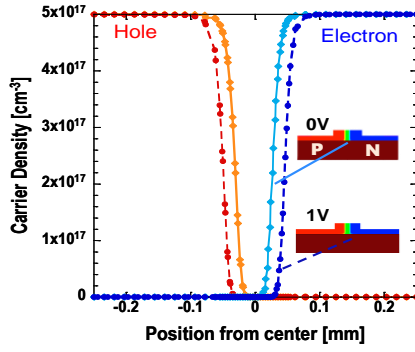


Fig. 3 Carrier distributions of electron and hole at 0V and 1V reverse bias voltage

3. Results of numerical analyses

Figure 3 shows carrier distributions of electron and hole in the InGaAsP optical modulator with a doping density of $5 \times 10^{17} \text{ cm}^{-3}$ when a reverse bias voltage is applied to the PN junction. As a reverse bias voltage increases, the depletion layer is widened as expected, resulting in optical modulation through the free-carrier effects in InGaAsP. Figure 4 shows the modulation efficiency $V_{\pi}L$ in the InGaAsP and Si optical modulators as a function of a reverse voltage. $V_{\pi}L$, which is a figure of merit of modulation efficiency, is defined by a product of bias voltage and device length required for π phase shift. When a bias voltage is 1 V, the $V_{\pi}L$ in the InGaAsP optical modulator is approximately 0.35 Vcm. As shown in Fig. 4 the InGaAsP optical modulator has five times smaller $V_{\pi}L$ than the Si modulator. The modulation efficiency improvement in the InGaAsP device is due to the greater electron-induced refractive index change in InGaAsP than in Si. The insertion losses caused by the carrier-induced absorption in the InGaAsP and Si devices are 0.89 dB/mm and 0.83 dB/mm, respectively. Despite the high modulation efficiency in the InGaAsP device, the insertion loss is comparable to that in the Si, meaning that the InGaAsP can greatly improve the trade-off between the modulation efficiency and insertion loss. Figure 5 summarizes the relationship between $V_{\pi}L$ and insertion loss in the carrier-depletion InGaAsP and Si optical modulators. Generally, when the doping density in a modulator is increased, the modulation efficiency improves, but at the

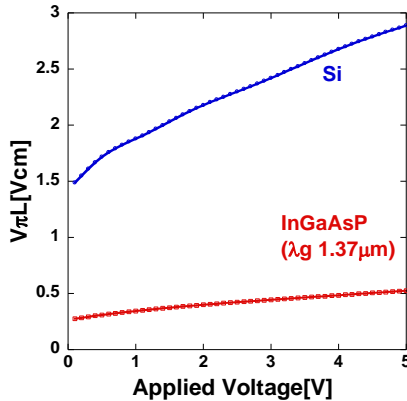


Fig. 4 Calculated $V_{\pi}L$ (Carrier density is $5 \times 10^{17} \text{ cm}^{-3}$)

same time the propagation loss increases. Hence the trade-off between the modulation efficiency and insertion loss cannot be improved in the Si modulators. On the other hand, as shown in Fig. 5, the InGaAsP can improve this trade-off owing to the large carrier-induced refractive index change. Thus, InGaAsP essentially improves the modulator performances as compared to Si.

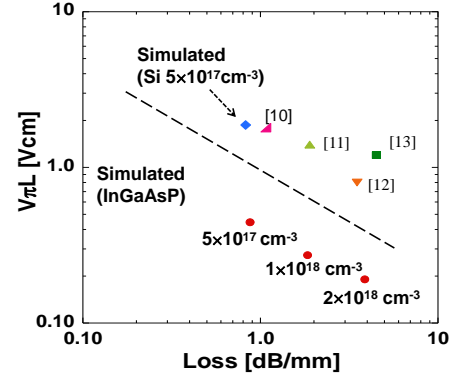


Fig. 5 Trade-off relationship between $V_{\pi}L$ and insertion loss.

4. Conclusion

We have numerically analyzed the modulation characteristics of the carrier-depletion InGaAsP optical modulator on the III-V CMOS photonics platform. Owing to the large electron-induced refractive index change in InGaAsP, the modulation efficiency is improved as approximately five times as compared with Si. Thus, the carrier-depletion InGaAsP optical modulator is promising for optical interconnections in datacenter networks.

Acknowledgement

This work was supported by a Grant-in-Aid for Young Scientists (A) from MEXT.

Reference

- [1] G. T. Reed et al., Nature photonics **4** (2010) 518-526.
- [2] R. Soref and B. R. Bennett, IEEE J. Quantum Electronics **23** (1987) 123-129.
- [3] M. Takenaka and Y. Nakano, Optics Express **15** (2007) 8422-8427.
- [4] M. Takenaka et al, Appl. Phys. Express **2** (2009) 122201.
- [5] M. Takenaka et al, Appl. Phys. Express **6** (2013) 042501.
- [6] Y. Ikku et al, Optics Express **20** (2012) B357-B364.
- [7] Y. Cheng et al, Jpn. J. Appl. Phys. **55** (2016) 04EH01.
- [8] S. Matsuo et al. Optics Express **22** (2014) 12139-12147.
- [9] B. R. Bennett et.al, IEEE J. Quantum Electronics **26** (1990) 113-122.
- [10] J. P. Weber, IEEE J. Quantum Electronics **30** (1994) 1801-1816.
- [11] X. Xiao et al. Optics Express **21** (2013) 4116-4125.
- [12] X. Xiao et al. Optics Express **20** (2012) 2507-2515.
- [13] H. Yu et al. Optics Express **20** (2012) 12926-12938.